

Magnon-Mediated Interactions between Fermions Depend Strongly on the Lattice Structure

Mirko Möller, George A. Sawatzky, and Mona Berciu

Department of Physics and Astronomy, University of British Columbia, Vancouver, British Columbia, Canada, V6T 1Z1
(Received 7 February 2012; published 23 May 2012)

We propose two new methods to calculate exactly the spectrum of two spin- $\frac{1}{2}$ charge carriers moving in a ferromagnetic background, at zero temperature. We find that if the spins are located on a different sublattice than that on which the fermions move, magnon-mediated effective interactions are very strong and can bind the fermions into low-energy bipolarons with triplet character. This never happens in models where spins and charge carriers share the same lattice, whether they are in the same band or in different bands. This proves that effective one-lattice models do not describe correctly the low-energy part of the two-carrier spectrum of a two-sublattice model, even though they may describe the low-energy single-carrier spectrum appropriately.

DOI: 10.1103/PhysRevLett.108.216403

PACS numbers: 71.10.Fd, 71.27.+a, 75.50.Dd

When studying properties of complex materials with ions on several sublattices it is customary to use simplified, one-lattice Hamiltonians to describe their low-energy physics. For example, instead of a two-sublattice model for the CuO_2 plane including both Cu $3d_{x^2-y^2}$ and O $2p$ orbitals [1], many prefer a one-band Hubbard model on the Cu (sub)lattice. States in this simpler model are Zhang-Rice singlets (ZRS), i.e., bound singlets between a hole at a Cu site and a doping hole delocalized over its four O neighbors with the same $d_{x^2-y^2}$ symmetry [2].

Such a composite object may describe well the low-energy quasiparticle, although this is still debated [3]. Less clear is whether a model based on such states that mix together charge and spin degrees of freedom, can properly describe quasiparticle interactions, especially those mediated through spin fluctuations. Most oxides have at least one phase with long-range magnetic order, and magnon exchange is believed by some to be a key component determining their properties, e.g., as the main “glue” for pairing in cuprates, which likely controls the value of T_c [4].

Here we show that effective one-lattice models severely underestimate the magnon-mediated attraction between carriers, compared to their two-sublattice “parent” model. The magnetic background is chosen as ferromagnetic (FM). This is much simpler than an antiferromagnetic (AFM) background, but it allows for exact solutions. Thus, any qualitative differences are inherent to the models themselves. Moreover, our conclusions are relevant to the modeling of carriers in AFM backgrounds, and raise serious questions about the ability of ZRS-like constructs to correctly describe low-energy, two-carrier states.

Our models are sketched in Fig. 1. For simplicity, we address the one-dimensional (1D) case; generalizations are straightforward. Model I is the “parent,” two-sublattice, two-band model. Model II is a two-band, single lattice effective model. Model III is an even simpler one-band effective model.

In models I and II, one band hosts the spin S degrees of freedom, described by

$$\mathcal{H}_s = -J \sum_i (\vec{S}_i \cdot \vec{S}_{i+1} - S^2).$$

This favors a FM ground state $|\text{FM}\rangle = | +S, \dots, +S\rangle$ for the undoped system. Spin- $\frac{1}{2}$ doping charge carriers occupy states in another band. In model I, this is located on a different sublattice, for example like in a CuO chain with spins on Cu and holes on O sites. In model II, they are on the same lattice. In both cases carriers are described by a Hubbard model

$$\mathcal{H}_c = -t \sum_{i,\sigma} (c_{i+1+\delta,\sigma}^\dagger c_{i+\delta,\sigma} + \text{H.c.}) + U \sum_i \hat{n}_{i+\delta,\uparrow} \hat{n}_{i+\delta,\downarrow},$$

where $\delta = \frac{1}{2}$ for model I, $\delta = 0$ for model II, $c_{i+\delta,\sigma}$ is the annihilation operator for a carrier of spin σ from site $i + \delta$, and $\hat{n}_{i+\delta,\sigma} = c_{i+\delta,\sigma}^\dagger c_{i+\delta,\sigma}$.

Interactions between charges and spins are described by the simplest exchange model. In model I, a carrier interacts with its two neighbor spins

$$\mathcal{H}_{\text{ex}}^{(I)} = J_0 \sum_i \vec{s}_{i+\frac{1}{2}} (\vec{S}_i + \vec{S}_{i+1}),$$

while for model II there is on-site exchange

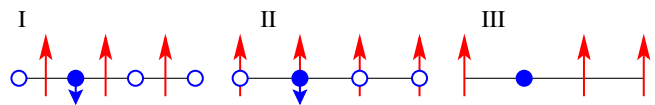


FIG. 1 (color online). Models I and II have two bands: one occupied by spins (arrows), and one (empty circles) hosting carriers introduced by doping (filled circles, with arrow showing the spin). In the “parent” model I, these are on different sublattices. In model II, they are on the same lattice. Model III has one band which hosts both spins (arrows) and ZRS-like polaron cores (filled circle).

$$\mathcal{H}_{\text{ex}}^{(\text{II})} = J_0 \sum_i \vec{s}_i \cdot \vec{S}_i.$$

Here $\vec{s}_{i+\delta} = \frac{1}{2} \sum_{\alpha, \beta} c_{i+\delta, \alpha}^\dagger \vec{\sigma}_{\alpha\beta} c_{i+\delta, \beta}$, where $\vec{\sigma}$ are Pauli matrices. We set $\hbar = 1$ and the lattice constant $a = 1$.

The one-band model III is described by the Hubbard Hamiltonian \mathcal{H}_c projected onto the appropriate subspace, e.g., $S_{\text{tot}}^z = NS - \frac{1}{2}$ if one spin down carrier is added.

We set $S = \frac{1}{2}$ (higher S is discussed elsewhere [5]), and first review the one-carrier case. If $\sigma = \uparrow$, the $T = 0$ problem is trivial in models I and II: spin flips are impossible; therefore, the eigenstates $c_{k\uparrow}^\dagger |\text{FM}\rangle$ have energy $E_{k\uparrow} = \epsilon_k + \gamma J_0$, where $\gamma = \frac{1}{2}$ ($\gamma = \frac{1}{4}$) in model I (II), and $\epsilon_k = -2t \cos(k)$ is the free carrier dispersion. Model III has a serious problem: it cannot distinguish an undoped system from one doped with spin up carriers.

The interesting case is for a carrier injected with spin down. In model III, this is trivial; the ‘‘hole’’ moves freely with energy ϵ_k . The exact solution (in any dimension) for the Green’s function $G_{\downarrow}(k, \omega) = \langle \text{FM} | c_{k,\downarrow} \hat{G}(\omega) c_{k,\downarrow}^\dagger | \text{FM} \rangle$ where $\hat{G}(\omega) = [\omega + i\eta - \mathcal{H}]^{-1}$ is the resolvent for $\mathcal{H} = \mathcal{H}_s + \mathcal{H}_c + \mathcal{H}_{\text{ex}}$, has long been known for model II [6]. Its generalization to two-sublattice models was proposed recently [7]. The off-diagonal part of \mathcal{H}_{ex} mixes $c_{k\downarrow}^\dagger |\text{FM}\rangle$, of energy $E_{k\downarrow} = \epsilon_k - \gamma J_0$, with the continuum of one-magnon states $c_{k-q\uparrow}^\dagger S_q^- |\text{FM}\rangle$ of energy $E_{k-q,\uparrow} + \Omega_q$. Here, $S_q^- = (1/\sqrt{N}) \sum_i e^{iqR_i} S_i^-$ is the magnon creation operator and $\Omega_q = 2J \sin^2(q/2)$ is the spin-wave dispersion. Also, $S_i^- = S_i^x - iS_i^y$ is the spin-lowering operator and $N \rightarrow \infty$ is the number of sites on either sublattice.

The interesting case is $J_0 > 0$: hybridization pushes the discrete state further below the continuum, resulting in a low-energy, infinitely lived quasiparticle (spin polaron), discussed next. If $J_0 < 0$, the low energy states are the incoherent continuum describing the scattering of the carrier off a free magnon [6]. One cannot further simplify the description of such states.

Returning to the spin polaron that is the low-energy quasiparticle for $J_0 > 0$, its structure can be understood in the limit $J_0 \gg t, J$. We start with model II. $\mathcal{H}_{\text{ex}}^{(\text{II})}$ is minimized by an on-site singlet between the carrier and its spin, $|s\rangle_i = (1/\sqrt{2})(c_{i\downarrow}^\dagger - c_{i\uparrow}^\dagger S_i^-) |\text{FM}\rangle$, with all other spins in the FM state. The energy of this degenerate state is $\mathcal{H}_{\text{ex}}^{(\text{II})} |s\rangle_i = -\frac{3}{4} J_0 |s\rangle_i$. Hopping lifts the degeneracy, and to first order in t, J , the polaron energy is

$$E_P^{(\text{II})}(k) \approx -\frac{3}{4} J_0 + \frac{1}{2} \epsilon_k + \frac{J}{2} \quad (1)$$

with $|P_{\text{II}}, k\rangle = (1/\sqrt{N}) \sum_i e^{ikR_i} |s\rangle_i$. Thus, the spin polaron is an on-site singlet between the charge and its local spin (or a bound state of the carrier with a magnon at the same site) that moves with an effective hopping $t/2$ suppressed

by the magnon cloud overlap. The last term is the FM exchange energy lost in the magnon’s presence.

Similar considerations apply to model I. Again, we only discuss the case $J_0 > 0$ which has a low-energy quasiparticle. Because of the two-sublattice structure, the ground state of $H_{\text{ex}}^{(\text{I})}$ is the three-spin polaron (3SP) $|3\text{SP}\rangle_{i+\frac{1}{2}} = [\sqrt{2/3} c_{i+\frac{1}{2}\downarrow}^\dagger - c_{i+\frac{1}{2}\uparrow}^\dagger (S_i^- + S_{i+1}^-)/\sqrt{6}] |\text{FM}\rangle$, of energy $\mathcal{H}_{\text{ex}}^{(\text{I})} |3\text{SP}\rangle_{i+\frac{1}{2}} = -J_0 |3\text{SP}\rangle_{i+\frac{1}{2}}$ [8]. It describes a bound state between the carrier and a magnon on either neighboring spin. Hopping lifts the degeneracy, resulting in $|P_{\text{I}}, k\rangle = (1/\sqrt{N}) \sum_i e^{ik(R_i+1/2)} |3\text{SP}\rangle_{i+\frac{1}{2}}$ with energy

$$E_P^{(\text{I})}(k) \approx -J_0 + \frac{5}{6} \epsilon_k + \frac{J}{6}. \quad (2)$$

In Fig. 2 we compare the exact spectra, calculated as in Refs. [6,7], with these asymptotic expressions (lines) for models I and II. The agreement is excellent for large J_0 and remains reasonable even down to $J_0 \sim t$, showing that this singlet or 3SP description of the spin polaron is robust. Figure 2(a) also shows another quasiparticle below the continuum. This is based on a higher eigenstate of $H_{\text{ex}}^{(\text{I})}$. (For more details, see [7]. Here we focus only on the low-energy physics.) Based on this, it is clear that if we are only interested in the low-energy spin down quasiparticle, we can map model I onto II and III, after some rescaling of parameters. The mapping from model I to II is obvious if we rewrite $|P_{\text{I}}, k\rangle = (1/\sqrt{2N}) \sum_i e^{ikR_i} [d_{k,i\downarrow}^\dagger - d_{k,i\uparrow}^\dagger S_i^-] |\text{FM}\rangle$, i.e., a singlet-type

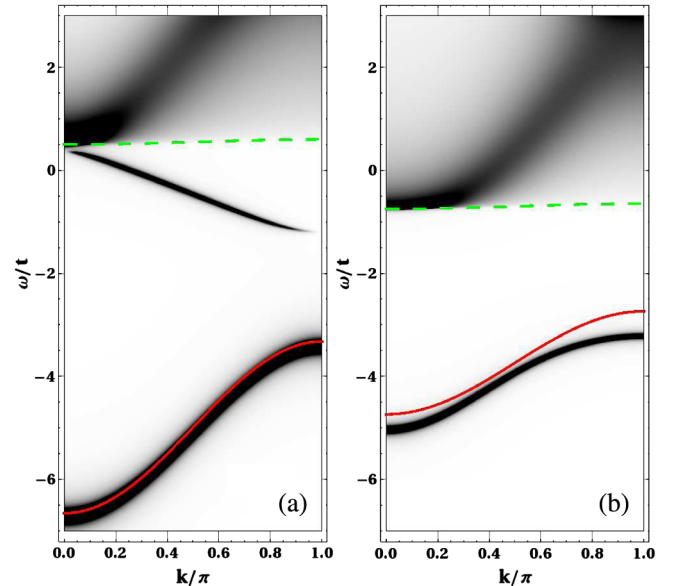


FIG. 2 (color online). (a) Model I, and (b) model II density of states $\rho_1(k, \omega) = -\frac{1}{\pi} \text{Im} G_{\downarrow}(k, \omega)$. Contour plots show exact results. Full lines are Eqs. (1) and (2), while dashed lines mark the expected onset of the continuum, at $\min_q(E_{k-q,\uparrow} + \Omega_q)$. Here $J/t = 0.05$, $J_0/t = 5$, $\eta/t = 0.02$.

state like $|P_{II}, k\rangle$, except that the carrier is in the “on-site” orbital $d_{k,i,\sigma}^\dagger = (1/\sqrt{3})(e^{ik/2}c_{i+\frac{1}{2},\sigma}^\dagger + e^{-ik/2}c_{i-\frac{1}{2},\sigma}^\dagger)$.

Thus, $|P_I, k\rangle$ is the direct analog of the ZRS: in the $k = 0$ ground state, the carrier occupies a linear combination of neighbor orbitals with the same s -type symmetry as the orbital giving rise to the S_i spin, with which it locks in a singlet. (If the orbitals had other symmetries, the hopping matrices would be different and the phases would change accordingly [7].) Like in the ZRS, $d_{k,i,\sigma}^\dagger$ is not orthogonal to its neighbor $d_{k,i\pm 1,\sigma}^\dagger$. Unlike the ZRS, these “on-site” states depend on k . This ensures the normalization of $|P_I, k\rangle$ in the entire Brillouin zone, unlike for the ZRS whose normalization diverges at $k = 0$ [2].

Nevertheless, if we ignore such complications and replace $d_{k,i,\sigma} \rightarrow c_{i\sigma}$, model I maps onto model II as far as the low-energy quasiparticle is concerned. Mapping to model III is the next step of replacing the ZRS with a “hole” which lives in the same band as the spins of the undoped system. Since model III has a quasiparticle band in the $S_{\text{tot}}^z = (N-1)\frac{1}{2}$ sector, it can also be mapped onto the quasiparticle band of model I, after rescaling.

The important question is whether this mapping between low-energy sectors carries on to cases with more carriers. We consider the two-carriers case, and show that model I has low-energy states which have no equivalent in models II and III. Specifically, magnon-mediated interactions can stabilize a low-energy bound pair in model I, if J_0 is sufficiently large. Such states never occur at low energies in model II, and are impossible in model III. This proves that modeling the proper lattice structure is essential to correctly describe magnon-mediated interactions.

The two-particle problem also has several cases. The trivial one is for two spin up carriers. In models I and II the carriers behave like non-interacting particles, with eigenstates $c_{k\uparrow}^\dagger c_{k'\uparrow}^\dagger |\text{FM}\rangle$ of energy $E_{k\uparrow} + E_{k'\uparrow}$. Model III does not distinguish this case from an undoped system.

The most interesting case is when one carrier is injected with spin up and the other with spin down. We analyze it in detail for models I and II, and then briefly discuss the case where both carriers are injected with spin down. We solve the problem exactly using two new methods.

The first method calculates two-particle Green’s functions in momentum space. Because of translational invariance, total momentum is conserved so nonvanishing matrix elements are $G(k, q, q', \omega) = \langle k, q | \hat{G}(\omega) | k, q' \rangle$, where $|k, q\rangle = c_{\frac{k}{2}+q,\uparrow}^\dagger c_{\frac{k}{2}-q,\downarrow}^\dagger |\text{FM}\rangle$ is a two-particle state with total momentum k . Momentum q is not conserved: on-site scattering changes it, as do magnon-mediated interactions. In the latter, the spin down carrier flips its spin creating a magnon, followed by absorption of the magnon by the other (initially spin up) carrier. The magnon’s momentum is, thus, transferred from one carrier to the other, and their spins are exchanged. It is precisely this effective interaction that interests us.

Because only one-magnon states are accessible from the original state, we obtain a closed system of equations of motion for these Green’s functions. This is rather similar to the single-carrier case [6,7]; however, the solution is now less trivial. In the Supplemental Material [9] we present the steps to reduce it to a closed equation that can be efficiently solved for a finite chain with $N \sim 100$. However, this becomes costly in higher dimensions, and may not generalize to other cases (e.g., more carriers).

We also propose a real-space solution for the infinite chain which allows us to find the symmetry of the pair (singlet vs triplet), and also generalizes to more carriers. It is based on the few-particle solution of Ref. [10]. Our case is more complex because when present, the magnon also counts as a “particle.” Thus, the system switches between having the carriers in states like $|k, n\rangle = (1/\sqrt{N})\sum_i e^{ik(R_i+\delta+\frac{\eta}{2})} c_{i+\delta,\uparrow}^\dagger c_{i+\delta+n,\downarrow}^\dagger |\text{FM}\rangle$ and three “particle” configurations $|k, n, m\rangle = (1/\sqrt{N})\sum_i e^{ik(R_i+\delta+\frac{\eta}{2})} c_{i+\delta,\uparrow}^\dagger c_{i+\delta+n,\uparrow}^\dagger S_{i+m}^- |\text{FM}\rangle$. Exchange connects propagators $G(k, n, n', \omega) = \langle k, n | \hat{G}(\omega) | k, n' \rangle$ to $G(k, n, n', m, \omega) = \langle k, n | \hat{G}(\omega) | k, n', m \rangle$, and vice versa. The solution of these equations is described in [9].

Poles of these propagators mark the two-carrier spectrum. Figure 3 shows $A(k, n, n', \omega) = -\frac{1}{\pi} \text{Im}G(k, n, n', \omega)$ for $k = 0$, $n = n' = 1$ and $J_0 = 20t$, chosen so large to simplify the task of identifying features.

The expected features in the spectrum of model I are the following. (i) A continuum describing states where the spin down carrier forms a polaron of momentum k' and the spin up carrier has momentum $k - k'$. These states span $\{E_P^{(1)}(k') + E_{k-k',\uparrow}\}_{k'}$ so the band edges are known from single-carrier results. Using Eq. (2) and ignoring small J

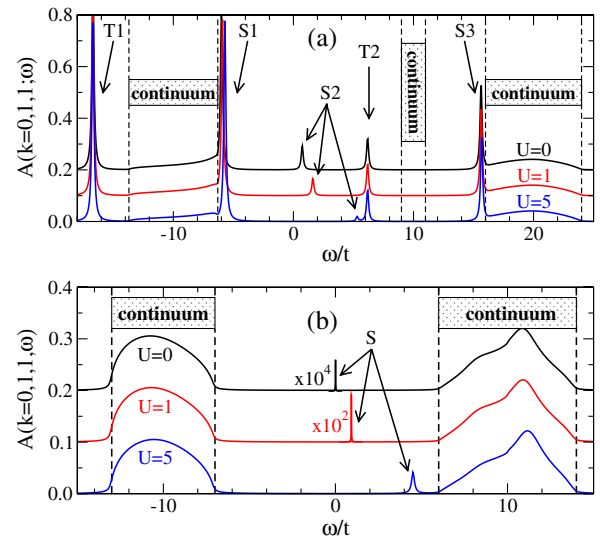


FIG. 3 (color online). Spectral weight $A(k = 0, n = n' = 1, \omega)$ for model I (a) and II (b). Expected continua locations are marked, as are triplet (T) and singlet (S) bipolarons (arrows). Here $J_0/t = 20$, $J/t = 0.05$, $\eta/t = 0.1$ and $U/t = 0, 1, 5$.

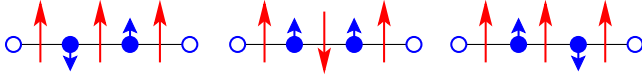


FIG. 4 (color online). The three highest weight configurations contributing to the low-energy bipolaron of model I.

corrections, the band edges are here expected at $-13.7t$ and $-6.3t$ (dashed lines), in good agreement with the results. (ii) A continuum $\{E_{k',\uparrow} + E_{k-k'-q,\uparrow} + \Omega_q\}_{k',q}$ describing states comprised of two spin up carriers and a free magnon. Expected band edges at $16t$ and $24t$ (dashed lines) show again good agreement. (iii) If there is a higher energy polaron state, like in Fig. 2(a), it will also generate a continuum. Here, its edges should be at $9t$ and $11t$. It is not seen in Fig. 3(a) because of vanishing overlap with the $|k=0, n=1\rangle$ state, but it appears in momentum-space Green's functions [9].

Any states outside these continua are bound states, “glued” through magnon exchange. Five such bipolarons appear in Fig. 3(a) (the apparent overlap between $S1$ and $S3$ with their nearby continua is due to the broadening $\eta = 0.1t$). For $k=0$, the real-space solution allows us to identify two as triplets and the others as singlets (see arrows). For finite k , there is no definite symmetry: these bound states have finite overlap with both singlet and triplet configurations, such as $\sum_i e^{ikR_i} (c_{i+\frac{1}{2},\uparrow}^\dagger c_{i+\frac{1}{2}+n,\downarrow}^\dagger \mp c_{i+\frac{1}{2},\downarrow}^\dagger c_{i+\frac{1}{2}+n,\uparrow}^\dagger) |FM\rangle$.

Consider now the low-energy bipolaron. Its largest overlap is with the configurations sketched in Fig. 4, hybridized through the J_0 exchange. It is the ability of both carriers to interact with *the same spin* to exchange the magnon, that stabilizes this state. This also explains why it is a triplet at $k=0$ (symmetric combination is favored), and its insensitivity to U : unlike singlets, triplets do not permit double occupancy. This bipolaron forms if $J_0/t > 6.5$, and is quite light [5].

Model II has different behavior; see Fig. 3(b). Again, a polaron + spin up carrier continuum, and a magnon + two spin up carriers continuum, are expected and observed. If J_0 is sufficiently large that the two do not overlap, a bound state appears between them, at $\omega \sim U$. This bipolaron is a singlet at $k=0$, quite similar to the $S2$ state in model I. It has very little weight in the $|k=0, n=1\rangle$ configuration, which is why we had to magnify the peaks. Most of its weight is on the on-site ($n=0$) configuration [9]. No tripletlike bound states appear, and no low-energy bipolaron is possible for any values of the parameters. This is not so surprising, since in this model only one carrier can interact with a given spin or magnon. If the carriers are on the same site they form a singlet which has no interactions with the local spin. If they are on neighboring sites, magnon exchange (now controlled by J , not by J_0 as in Fig. 4) is too weak to stabilize a low-energy bipolaron. Thus, model II simply cannot describe the low-energy physics

of model I in this sector. Model III fails as well, since it does not distinguish between a spin up carrier and a lattice spin.

We also considered the two spin down carrier states. For models I and II, the $t=0$ solutions suggest that the lowest energy feature is the two-polaron continuum. This is reasonable, since each carrier can bind its own magnon to create a polaron. Simultaneous interaction of one carrier with two magnons is impossible in model II, and while possible, it is energetically unfavorable in model I, so low-energy bipolarons do not appear in this sector. Turning on hopping further favors the continuum, since polarons are lighter than a bipolaron [5]. In model III, no interactions are possible between two “holes”, since they simply reshuffle the FM spins as they move. This is why we have not investigated this case in more detail.

To summarize, we extended the exact solution for a single charge in a FM background to cases with two or more carriers, and discussed in detail the nontrivial case where one carrier is injected with spin up and the other with spin down. The low-energy physics depends essentially on the model. If the spins are intercalated between the carrier sites, magnon exchange is enhanced and can bind low-energy bipolarons. If spins and carriers live on the same lattice, such low-energy states are impossible. If spins and carriers live in the same band, there are no magnon-exchange interactions in any of the allowed cases. These three models have very different low-energy states in the two-particle sector, even though their one-particle sectors can be mapped onto one another.

This shows that in order to properly describe magnon-mediated interactions, one must use the proper sublattice structure, not simpler effective one-lattice models. While our work is for a FM background, it is directly relevant for AFM backgrounds as well, since the magnon exchange is a rather local process. Based on our results, for a CuO_2 lattice one should expect strong magnon-mediated interactions between two holes located at neighbor O sites, through their common Cu (the 2D analog of Fig. 4). A one-band model based on ZRSs simply cannot describe this process, and is therefore likely to severely underestimate the role of magnons as the “glue” for pairing.

This work was supported by NSERC, QMI, and CIFAR.

-
- [1] V.J. Emery, *Phys. Rev. Lett.* **58**, 2794 (1987).
 - [2] F.C. Zhang and T.M. Rice, *Phys. Rev. B* **37**, 3759 (1988).
 - [3] B. Lau, M. Berciu, and G.A. Sawatzky, *Phys. Rev. Lett.* **106**, 036401 (2011); B. Lau, M. Berciu, and G.A. Sawatzky, *Phys. Rev. B* **84**, 165102 (2011).
 - [4] See T. Dahm, V. Hinkov, S.V. Borisenko, A.A. Kordyuk, V.B. Zabolotnyy, J. Fink, B. Büchner, D.J. Scalapino, W.

- Hanke, and B. Keimer, *Nature Phys.* **5**, 217 (2009), and references therein.
- [5] M. Möller, G. A. Sawatzky, and M. Berciu (unpublished).
- [6] B. S. Shastry and D. C. Mattis, *Phys. Rev. B* **24**, 5340 (1981).
- [7] M. Berciu and G. A. Sawatzky, *Phys. Rev. B* **79**, 195116 (2009).
- [8] V. J. Emery and G. Reiter, *Phys. Rev. B* **38**, 4547 (1988).
- [9] See Supplemental Material at <http://link.aps.org/supplemental/10.1103/PhysRevLett.108.216403> for further details.
- [10] M. Berciu, *Phys. Rev. Lett.* **107**, 246403 (2011).